Proceedings of Global Power and Propulsion Society
ISSN-Nr: 2504-4400
GPPS Hong Kong 2023
October 17-19, 2023
www.gpps.global

# GPPS-TC-2023-0044

# FAST ASSESSMENT OF TURBINE BLADE PERFORMANCE WITH NON-UNIFORM BOUNDARY CONDITION USING ADJOINT SENSITIVITY

**Kexin Hu**
**Tsinghua University**
hkx21@mails.tsinghua.edu.cn
Beijing 100084, P.R. China

**Zhen zhang**
**Tsinghua University**
zhen@mail.tsinghua.edu.cn
Beijing 100084, P.R. China

**Xinrong Su**
**Tsinghua University**
suxr@mail.tsinghua.edu.cn
Beijing 100084, P.R. China

**Xin Yuan**
**Tsinghua University**
yuanxin@mail.tsinghua.edu.cn
Beijing 100084, P.R. China

## ABSTRACT

In modern gas turbine engines there exist significant temperature gradients in the combustor exit. The temperature non-uniformity makes it difficult to predict turbine blade performance quickly. The computational method of fully coupled combustor-turbine can be used to accurately simulate the flow field at the combustor exit and predict turbine performance, but the method is complex and the computational cost is extremely high. In this study, a turbine blade performance prediction method based on using adjoint sensitivity is proposed, which can take turbine performance, such as mean temperature of the blade surface, as observables to calculate the sensitivity to the boundary conditions. Based on the sensitive information, the observable under the non-uniform inlet can be quickly predicted. The accuracy of this prediction method can be satisfied to the needs of industry design and reduces the computational cost of the simulation.

## INTRODUCTION

In modern aero-engine and gas turbine, the interaction between the combustor and the turbine has a significant impact on the aerodynamic and cooling performance of the turbine. Due to the presence of residual swirl and hot streak, the distribution of velocity, temperature, and turbulence of the turbine inlet are highly nonuniform. The hot streak not only cause localized hot spots on the vane surfaces but also influence the flow field of rotor passage especially the tip region(Simone et al. 2012). Basol et al (Basol et al 2011) analysed the migration pattern of the hot streak and discussed the underlying mechanisms. They found reduction in the rotor blade tip adiabatic wall temperatures could be achieved by changing the clocking the hot streak. That means the aerodynamic performance of the turbine can be influenced by the design of the position of hot streak. Li et al. (Li et al., 2019) focused on the different design philosophies of combustors and turbines. The results indicate that the non-uniformity clocking position dominates the average temperature and emphasize the necessity of considering the mismatching effect in gas turbine design optimization. Generally, researchers use experimental or numerical methods to study the turbine performance under typical non-uniform inlet conditions. Idealized round hot streak is often used in earlier simulation studies because of its simple structure and easy quantification. Feng et al. (Feng et al. 2016) use the temperature profiles with hot streak are set as parabolic curves in radial and circumferential directions to simulate the turbine inlet conditions. An et al. (An et al. 2009) used the simple 2D contours of the inlet total temperature to simulate the exit temperature field of combustor and changed the circumferential positions of the hot streak to explore the hot streak migration in vane passage and paid attention to the transient heat load variation. While Zakaria and Richard (Zakaria and Richard 2022) found the actual condition in turbine is far more complicated than the ideal hot streak and swirl. Some researchers use experiments to simulate the non uniform inlet conditions or research based on the real machine measurement results (Povey et al. 2005 Jenny et al. 2012). In order to obtain more accurate turbine inlet conditions, some researchers choose to use numerical calculations to simulate the interaction of combustor and turbine (Miki et al. 2022, Wang et al. 2023).

Based on the studies about effects of hot streak on flow and heat transfer characteristics of turbine, how to optimize the relative position of inlet guide vane (IGV) and non-uniform boundary conditions to obtain better performance becomes a problem worth considering. Although these methods can obtain accurate cooling and heat transfer data for mechanism analysis, but they are not suitable for industrial optimization design due to high cost of simulation or experiments. If the gradient information can be obtained based on a small number of calculations for a variety of non-uniform boundary conditions, it will greatly simplify the optimization design considering mismatching effect in turbine design. Adjoint solver is not a new method used in the turbine researches. However, many researches are mainly pay attention to realization of adjoint solver (Jacques and Richard, 2010) or using it to optimize the blade profile (such as Lu et al. 2013, Gustavo et al. 2020, Arens et al. 2005). In a typical aerodynamic shape design optimization problem for turbine cascades, the objective function is usually set as an aerodynamic parameter and combine FFD or other curves to describe the geometry of blade, obtain a better blade or indicating the ability and efficiency of the design optimization system based on adjoint method in the field of the turbine cascades. While the sensitivity information provided by adjoint solver can also be used to analyse the influence of non-uniform boundary condition. Su and Yuan (Su and Yuan, 2022) first use adjoint method to study the sensitivity of the inlet boundary conditions. Zhang et al. (Zhang et al. 2022) proposed an efficient method to study the influence of non-uniform boundary conditions by sensitivity obtained by discrete adjoint method.

In this paper, the adjoint method is used to obtain the sensitivity of boundary condition which can predict the observable under non-uniform inlet conditions. The calculation accuracy can be satisfied to the needs of industry design and reduce the computational cost. The relationship between sensitivity to boundary condition and flow fields is also attempted to be explained in this paper.

## NUMERICAL METHODS

The adjoint calculation is completed based on the discrete Adjoint Solver built in Fluent. The Adjoint Optimization toolbox has been used in designing optimized geometry of film cooling holes and the validity of this method have been demonstrated (Jones et al. 2021). An observable is created after computing the flow solution using RANS and activating the adjoint solver. The stabilization of the adjoint system solver was achieved by using the default settings, which have been proven to be robust and reliable. Sensitivities play a crucial role in gradient-based shape optimization for general adjoint optimization processes. Understanding these sensitivities in a fluid system can provide useful engineering insights. The computing details of the Adjoint Solver can be found in the Ansys Fluent Users Guide, so we will not delve too deeply into describing the solution process and equations of the discrete adjoint solver.

Flow solution is calculated using RANS method with realizable k-epsilon as model and enhanced wall treatment as near-wall treatment. The inlet boundary condition is set as velocity inlet with 5% turbulent intensity and turbulent length scale is set as axial chord length. In order to verify the accuracy of flow fields calculations, the static pressure on vane surface with an inlet velocity 12m/s and a temperature of 300K as boundary condition is compares with experimental measurements as shown in Figure 1. The experiment was finished in a low speed wind tunnel at Tsinghua University (Zhang et al. 2019). The same inlet condition is used in a cascade and measured the static pressure in an isometric vane using a differential pressure gauge. A good agreement between the numerical results and experimental data confirms the reliability of the computational solution.

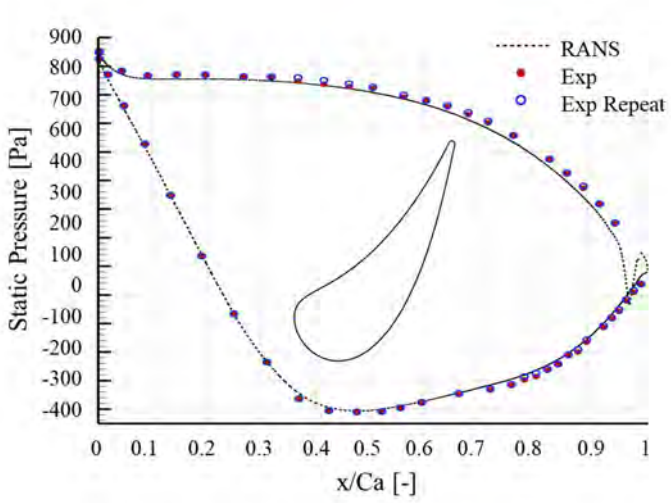


**Figure1 The vane profile and comparison of RANS and experiment**

Figure 2 shows the vane geometry both 2D and 3D used in this research. In order to obtain a reliable numerical solution as the reference, the grid independence verification was carried out firstly. The area weighted average temperature of vane is set as observable. The Results from the grid independence test is shown in Figure 3. The value of vertical axis is the

sensitivity on cells of inlet boundary divided by the cell length in the y direction. So the integral of the curve with respect to horizontal axis means when the condition temperature uniformly increase 1K then the observable will increase 1K. For convenient comparison, in 3D case we integrate the values of sensitivity in the z direction (the height direction of vane) so that the area of the curve surrounding the horizontal axis still has the same meaning with 2D cases. Finally the mesh a 2D mesh with size of 115 thousands and a 3D mesh with size of 923 thousands are selected as the computational mesh.

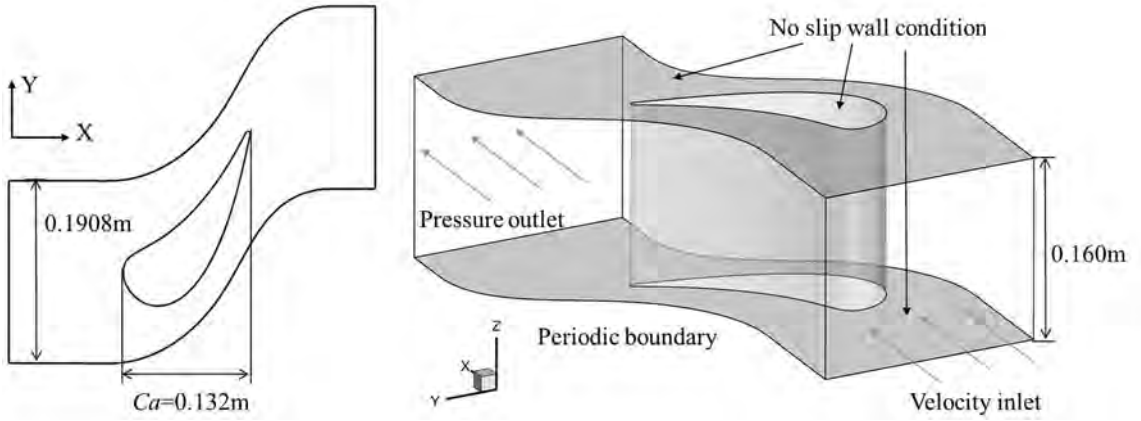


**Figure 2 The inlet guide vane geometry**

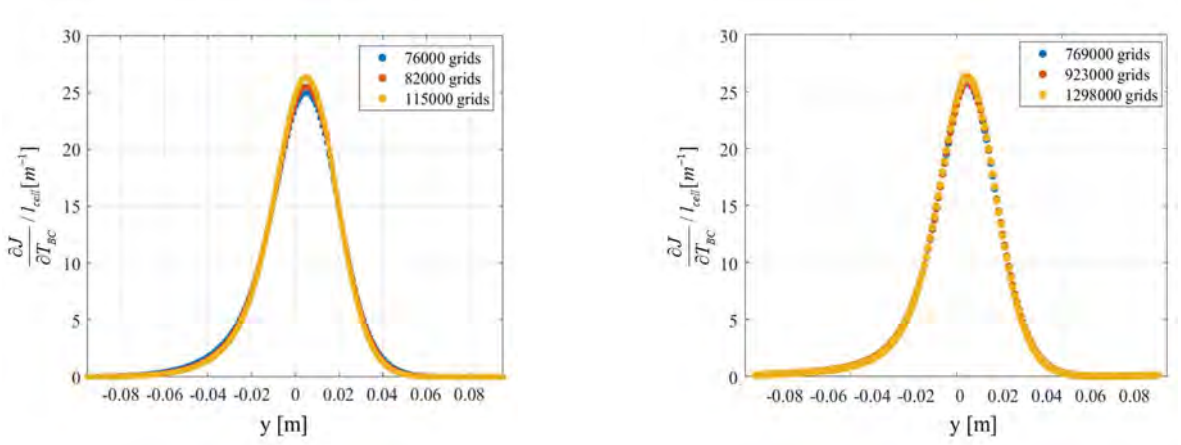


(a) 2D cases (b) 3D cases

**Figure 3 Sensitivity of objective to boundary temperature on different meshes**

Calculation time is an important part which base on the mesh, boundary condition and computational condition. For the cases in the study, the time of adjoint solver is approximately equal to RANS. 56 processes were used for parallel computing and the 2D cases use about 5 minutes while the 3D cases use about 7 hours for completion.

## SENSITIVITY IN DIFFERENT BOUNDARY CONDITION

The robust performance of the sensitivity of boundary condition on different temperature inlet is firstly verified. Figure 4 shows the sensitivity on boundary condition under three temperature profile: 300K uniform inlet, 300K sinusoidal temperature inlet and 600K uniform temperature inlet, when the area-averaged temperature of vane is set as observable $J = \bar{\bar{T}}_{vane}$. The coordinate position y corresponding to the sensitivity peak is not zero, which means the most sensitive position is not directly opposite the geometric leading edge point, but near the pressure surface. Though there are subtle differences in the curve in Figure.4, but the relative error is less than 3%. The conclusion can be drawn that the sensitivity of the observable to temperature boundary condition does not change when only the inlet temperature changes over a large temperature range (e.g. 300K~600K).

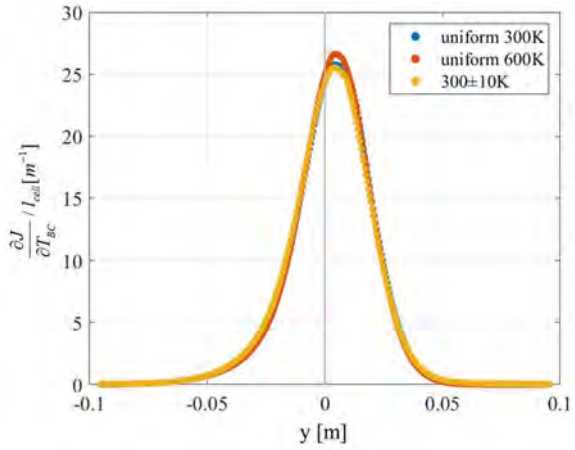


**Figure 4 Sensitivity to boundary temperature in different inlet temperature profile**

This robustness indicates that the observable at any non-uniform temperature distribution (within a range) can be predicted by relying only on the sensitivity information obtained from the adjoint calculation of one uniform temperature inlet when the velocity boundary conditions are constant. This conclusion can also be explained from the perspective of flow field. In the range of temperature variation used in the study, the density change caused by temperature as while as the influence on flow field can be basically ignored. Thus the sensitivity information is similar under non-uniform temperature inlet.

On the basis of this conclusion, in order to verify the accuracy of the adjoint method, sinusoidal temperature inlet conditions are set at the inlet: The temperature T and the variation dT can be described as:

$$T_{BC} = A + k\sin(\frac{2\pi}{l}(y+\varphi)) \qquad (1)$$

$$dT_{BC} = A + k\sin(\frac{2\pi}{l}(y+\varphi)) - 300 \quad (2)$$

where the pitch $l$=0.1908m in these cases and y is the coordinate. Different A, k and φ is chosen to get different T distribution. The velocity inlet is 12m/s. The prediction process based on boundary sensitivity is as follows:

$$dJ = \int_{inlet} \frac{\partial J}{\partial T_{BC}} dT_{BC} \qquad (3)$$

where $J = \bar{\bar{T}}_{vane}$ is the observable and dJ is the variation of J compared with the base line with the boundary condition in the uniform temperature 300K. The dJ obtained by RANS and the prediction calculated by sensitivity information are shown in Figure 5, indicating that the sensitivity has a satisfying prediction accuracy in a certain temperature range.

The boundary sensitivity information simplifies the prediction of the observable under the non-uniform temperature inlet. For the sinusoidal temperature distribution with the same cycle of vane passage, when the highest or lowest temperature point located at y=0.003m on inlet where corresponding to a position to the pressure surface of vane, the area average temperature of vane is the highest or the lowest. This conclusion indicates that when designing a turbine cascade, it is helpful to ensure the peak temperature is located in the location with low temperature boundary sensitivity if considering the matching relationship between the non-uniform temperature distribution and vane position is needed. The sensitivity to the boundary temperature can provide reliable predictions for non-uniform inlet temperature conditions.

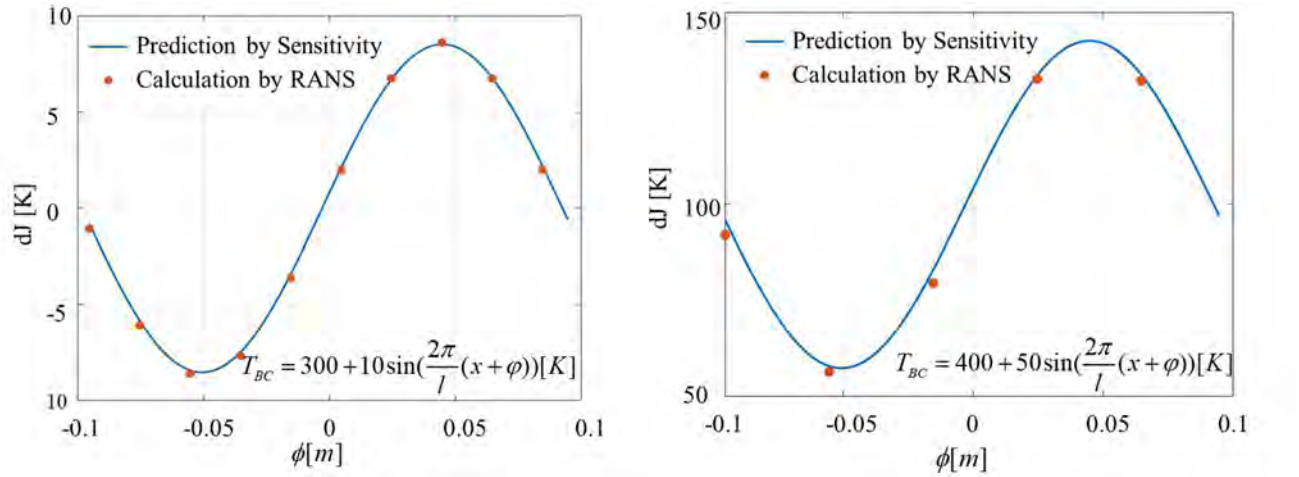


**Figure 5 Comparison of calculation and prediction in different inlet temperature profile**

For this 2D case, changing the inlet y velocity means changing the inlet flow angle. In the range of flow velocity U in 10~20 m/s and circumferential velocity V in-5~5 m/s, 50 points are randomly sampled. The distribution of sampling points is shown in the figure 6 and the point of base line is coloured red.

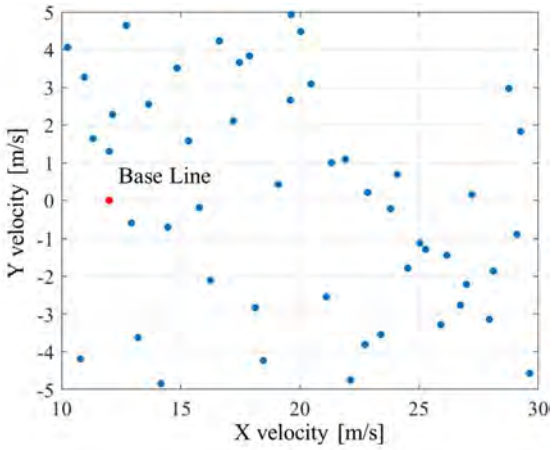


**Figure 6 The distribution of samples in the velocity space**

The boundary temperature sensitivity is calculated by the observable $J = \bar{\bar{T}}_{vane}$, and the results are shown in the figure 7(a), and the red points are the reference value. It can be found from the figure 7(a) that the sensitivity distribution under different velocity inlet conditions has a certain regularity. Then we extracted the y coordinate of the stagnation streamline at the inlet boundary and use them to translate the sensitivity curves in figure 7(a) to make these y position correspond to the zero of horizontal axis. The results are shown in the figure 7(b). The translated curves are approximately coincident, and the peak value is approximately near zero, which indicates that the peak of sensitivity is related to the inlet position of the stagnation streamline even when the inlet flow angle changes.

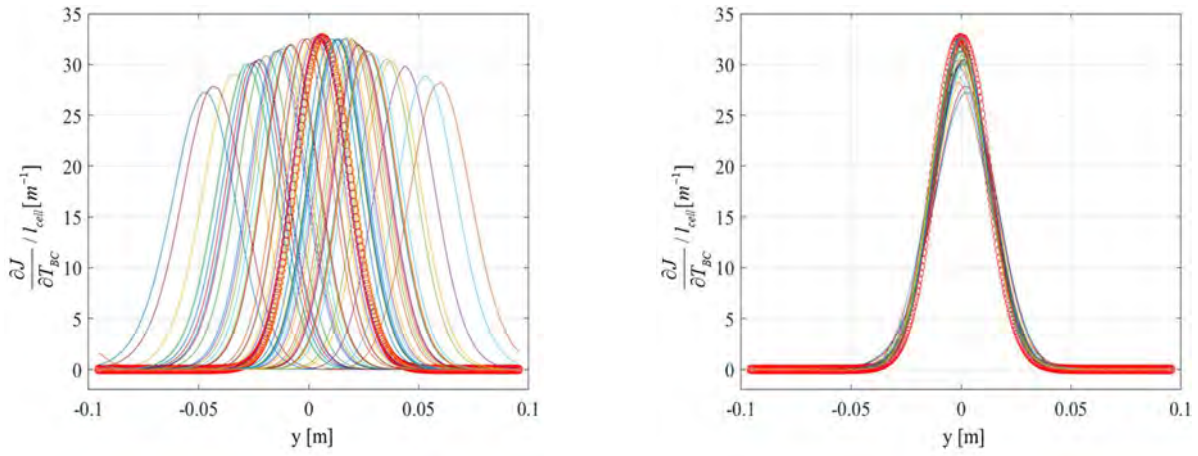


(a) original data

(b) translated by the y coordinate of stagnation streamline inlet position

**Figure 7 The sensitivity to boundary temperature under different velocity inlet The base line is marked by red circle.**

The curves in Figure7 can be fitted with normal distribution as equation (4):

$$\frac{\partial J}{\partial T_{BC}} l_{cell} = \frac{1}{\sigma\sqrt{2\pi}} \exp\left(-\frac{(x-\mu-y_{streamline})}{2\sigma^2}\right) \qquad (4)$$

where $y_{streamline}$ is y coordinate of stagnation streamline inlet position which used in Figure 7(b). The parameters R-square which are used to evaluate the goodness of fit are all over 0.998. Figure 8 shows the distributions of fit coefficients vary different inlet parameters. The inlet flow angle is computed as equation (5).

$$\varphi = ac\tan\frac{v}{u} \times \frac{180}{\pi} \qquad (5)$$

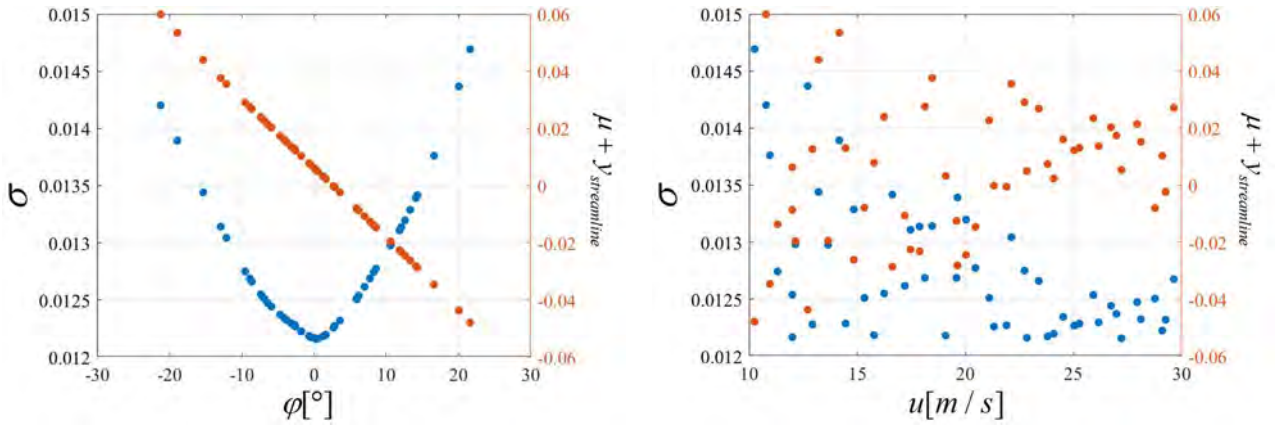


**(a) inlet flow angle as axis** **(b) X velocity as axis**

**Figure 8 Distribution of inlet flow parameters and fit coefficients**

Figure 8 shows the shape of sensitivity curves is strong correlated with the inlet flow angle, not the inlet flow velocity. That means when using normal distribution to fit the curve, the coefficients, σ and $\mu + y_{streamline}$, can be can be computed parametrically by flow angle. Based on this finding, we can obtain the sensitivity curve under other inlet conditions by transform the base line. In order to further study the relationship between sensitivity distribution and velocity boundary conditions, flow fields under the base line case and three inlet conditions which are random selected are used to observe, as shown as figure 9. The streamline corresponding to the position with sensitivity of boundary temperature is 0.3 are coloured blue, and purple streamline represents the stagnation streamline. The high sensitivity area corresponds to the streamlines around the vane, and the change of streamline caused by the inlet flow angle directly causes the translation and scaling of the sensitivity to the boundary temperature.

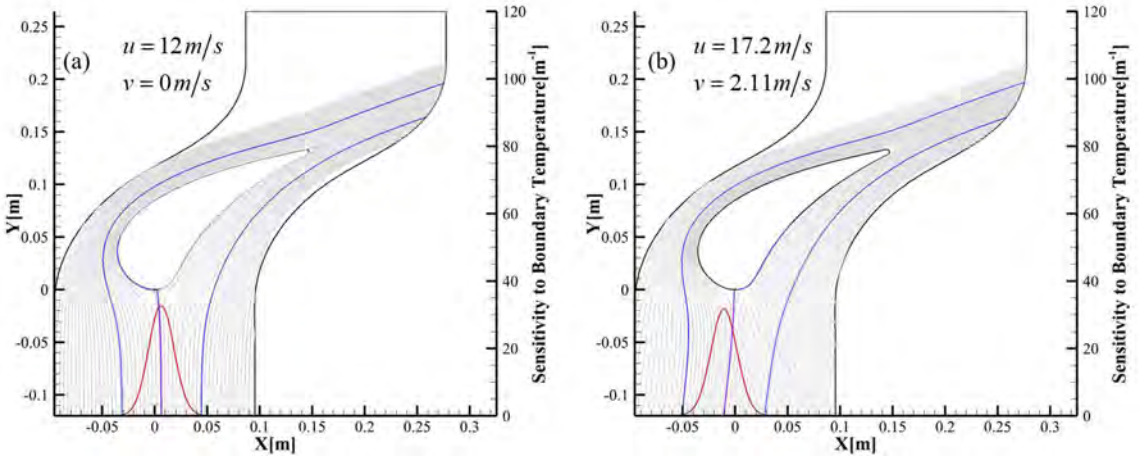

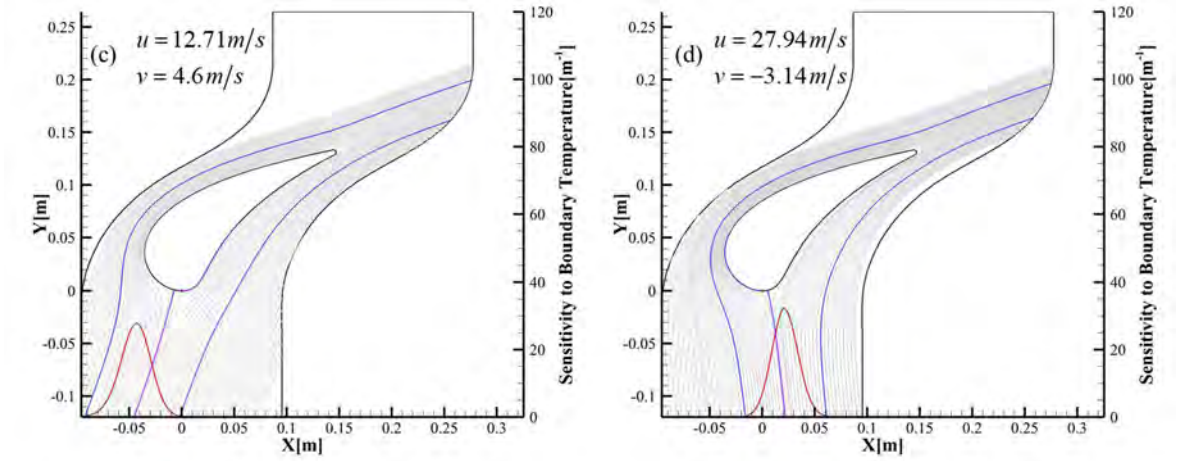


**Figure 9 The streamline and sensitivity to the boundary temperature in different velocity condition**

In addition, the distribution of sensitivity to boundary condition in 3D cases is studied. Same as the 2D cases, the inlet velocity is 12m/s normal to the boundary, and the temperature is 300K and the observable $J = \bar{\bar{T}}_{vane}$. Figure 10(a) shows the sensitivity to boundary temperature distribution on the inlet and the unit is m^-2 to ensure $\iint (\frac{\partial J}{\partial T_{BC}} / A_{cell}) ds_{BC} = 1$ which means when the inlet uniformly increase 1K the area-averaged temperature of vane will increase 1K. Similar to the 2D case, the peak of sensitivity is closer to the pressure surface (where the y coordinate is above 0[m]). But near the endwall with y position range -0.07m~-0.03m there is a strip of high sensitivity area, which is significantly different from the mid-span (x=0.08m). The cause of this region can be found in the flow filed as figure 10(b) shows. A slice near the trailing edge is extracted and coloured by x vorticity. Streamlines with positive x vorticity are coloured red, while negative x vorticity are coloured blue, and streamlines from high sensitivity region are coloured orange. It can be found that the blue streamlines come from the higher sensitivity region near the endwall, which means the region in high sensitivity is caused by a branch of the vortex pair near the trailing edge. The red streamlines correspond to the high sensitive area of the leading edge, and the orange streamlines come from the most sensitive inlet area and flow around the vane. The distribution of the sensitivity can provide an advice: It will be helpful to avoid putting high temperature areas on the leading edge region or the endwall region near suction surface.

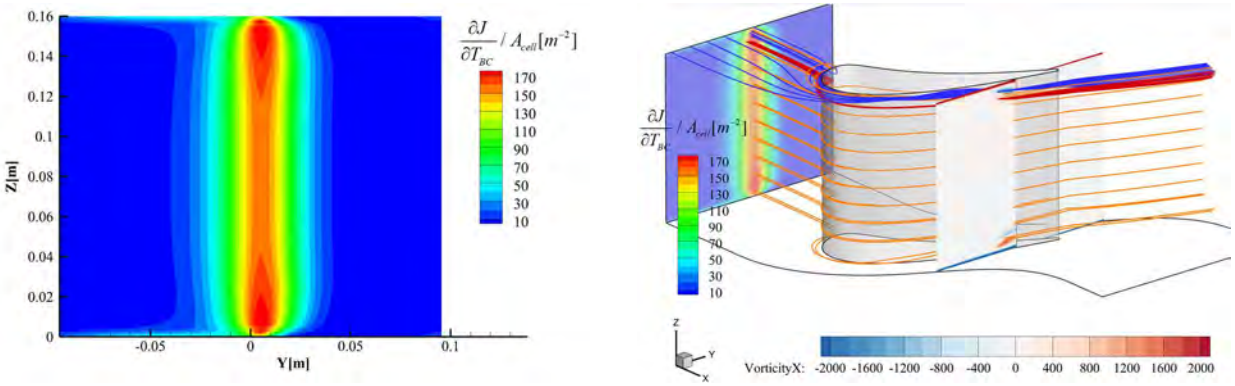


(a)Sensitivity to the boundary temperature (b) Streamlines and slice coloured by x vorticity

**Figure 10 The distribution of sensitivity and flow filed of uniform inlet condition**

In order to verify the accuracy of the boundary sensitivity of the 3D cases, three hot streaks distributed by the quadratic function with radius 0.8m are used. The inlet temperature is shown in the figure 11.

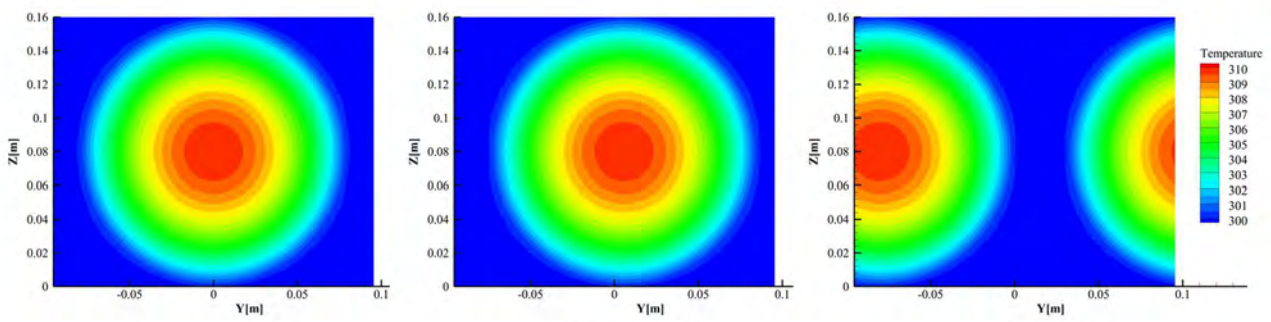


(a)Hot streak 1 (b)Hot streak 2 (c)Hot streak 3

**Figure 10 Three hot streaks inlet profile**

The observable is calculated by RANS when only the inlet temperature condition is changed. The prediction calculation based on sensitivity to boundary temperature is:

$$dJ_{per} = \iint_{inlet} \frac{\partial J}{\partial T_{BC}} dT_{BC} \quad (6)$$

The absolute and relative errors of the calculated and predicted values are compared. The calculation results of the location parameters and observed values of the hot streak core are shown in the Table 1. It can be seen that the absolute error of the prediction method is about 0.6% for hot streak 1, which is directly facing the geometric leading edge, and hot streak 2, which is close to the sensitivity maximum position. But the relative error of hot streak 3, which is located at the passage, is much larger. We thought as the value of the J is closer to the base line and dJ is closer to 0, so the error of prediction is higher. The same conclusion can be drawn that the prediction method based on boundary sensitivity can achieve satisfactory accuracy for non-uniform temperature inlet conditions in 3D cases.

**Table1 Parameters of hot streak and comparison of RANS and prediction**

| | Center of hot streak | | observable | | | | |
|---|---|---|---|---|---|---|---|
| | x/m | y/m | $J = \bar{\bar{T}}_{vane}$ | $dJ_{RANS}$ | $dJ_{pre}$ | $dJ_{pre} - dJ_{RANS}$ | $\frac{dJ_{pre} - dJ_{RANS}}{dJ_{RANS}}$ |
| uniform | \ | \ | 299.7021 | \ | \ | \ | \ |
| hot streak1 | 0 | 0.08 | 305.9016 | 6.1995 | 6.1599 | -0.64% | 0.0396 |
| hot streak2 | 0.00572 | 0.08 | 305.9098 | 6.2077 | 6.1702 | -0.60% | 0.0375 |
| hot streak3 | -0.08 | 0.08 | 300.1581 | 0.4560 | 0.5211 | 14.28% | -0.0651 |

However, for the 3D case of non-uniform velocity inlet, the boundary condition sensitivity is not as regular as the 2D case. The Y and Z velocity conditions with sinusoidal distribution are provided to simulate the swirl inlet. Swirl 1 has the core directly towards the geometric leading edge point, and swirl 2 directly towards the passage centre. Figure 12 shows the inlet sensitivity and streamlines under two swirling conditions. The streamlines are the same colour as the figure 11(b). The sensitivity distribution of inlet is greatly different from that of uniform velocity inlet, but the corresponding relationship between the locations of streamlines inlet and boundary sensitivity still exists. That is, the high sensitive area corresponds to the streamlines around the blade surface, and the high sensitivity area near the endwall corresponds to the branch of the passage vortex near the trailing edge.

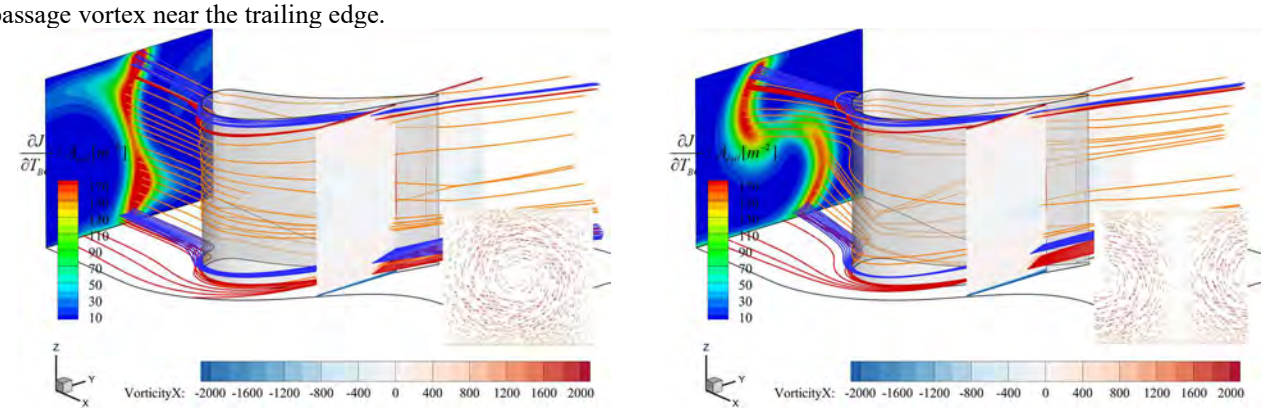


(a)Swirl 1 (b) Swirl 2

**Figure 12 The distribution of sensitivity and flow fields of non-uniform inlet condition**

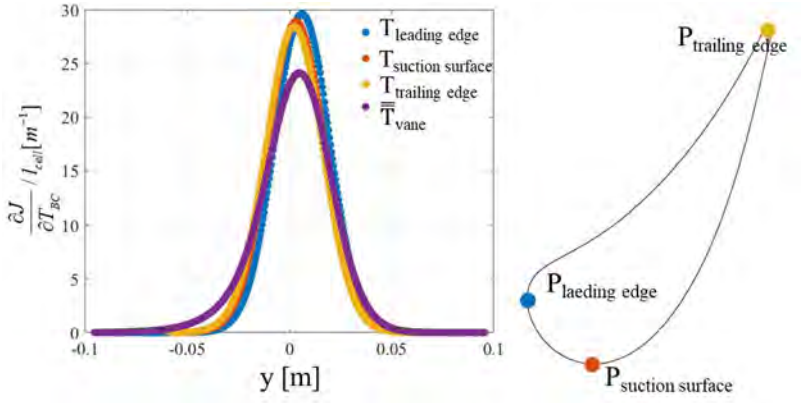


**Figure 13 The sensitivity curves with different observable and the position of the three points**

Usually the temperature of particular points on the vane surface is also a problem that is paid attention to. Therefore, in the following 2D cases, we set the temperature of the three points and $\overline{\overline{T}}_{vane}$ as observable, and study the sensitivity to boundary temperature. Figure 13 shows the points on vane surface which are point on leading edge (LE), point on suction surface(SS), point on trailing edge(TE) and the sensitivity when the temperature of them are set as observable. The peak value and width of the curve differ from the position of the point which indicates the temperature of different position on vane are affected differently by the inlet temperature change.

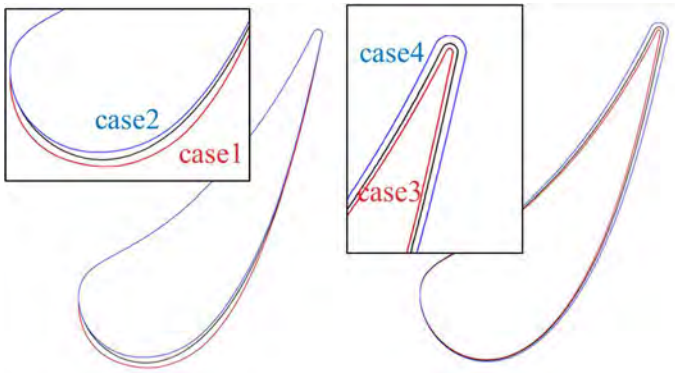


**Figure 14 The diagrams of four geometries (original geometry is black line)**

Since the sensitivity information can describe the robustness of vane temperature to boundary condition, then how does the sensitivity information differ for different vane geometries. In a design problem, if we have known the inlet condition as the combustor has already been designed, whether we can design a vane, which has less influence by the non-uniform inlet temperature, based on the sensitivity information. Four geometries are drawn by CAD to test the sensitivity to boundary temperature of different vane geometry. Case 1 and 2 change the radius of trailing edge while case 3 and case 4 change the thickness of suction surface which are shown in figure14. Normal curves, as equation (7) shows, are used to fit the sensitivity to boundary temperature on different observable and all the value of r-square are above 0.995.

$$\frac{\partial J}{\partial T_{BC}} l_{cell} = \frac{1}{\sigma\sqrt{2\pi}} \exp\left(-\frac{(x-\mu)}{2\sigma^2}\right) \qquad (7)$$

As the σ describes the location of peak value and the μ describes the width in a normal curve, we can compare the robustness of observable to boundary condition by σ and the inlet position with the highest sensitivity by μ. The relative error to the fit coefficients of original geometry which is calculated by: $E_\sigma = \frac{\sigma-\sigma_{originale}}{\sigma_{originale}}$ and $E_\mu = \frac{\mu-\mu_{originale}}{\mu_{originale}}$ are shown in Figure 15. The relative error evaluates the change of the sensitivity to different objective, comparing with the base line geometry. High error means the vane shape's deformation causes large difference to the sensitivity to boundary temperature and the low error means the opposite. Firstly we can find in Figure 15 that the absolute $E_\sigma$ for different cases and observables are under 2% but case 1 has higher value than others which indicates larger leading edge or thicker suction surface may reduce the influence of non-uniform inlet temperature on heat load, especially at key positions such as leading edge points. The absolute $E_\mu$ may be higher than 50% means the differences on the position of highest sensitivity may be significant. Case 1 and case 2 have higher $E_\mu$ than case3 and case 4 shows the change on the thickness of suction surface have more influences on the μ. If there is a hot streak directly opposite the leading edge, then modifying the suction surface thickness is more beneficial to reducing the heat load on vane surface than modifying the trailing edge.

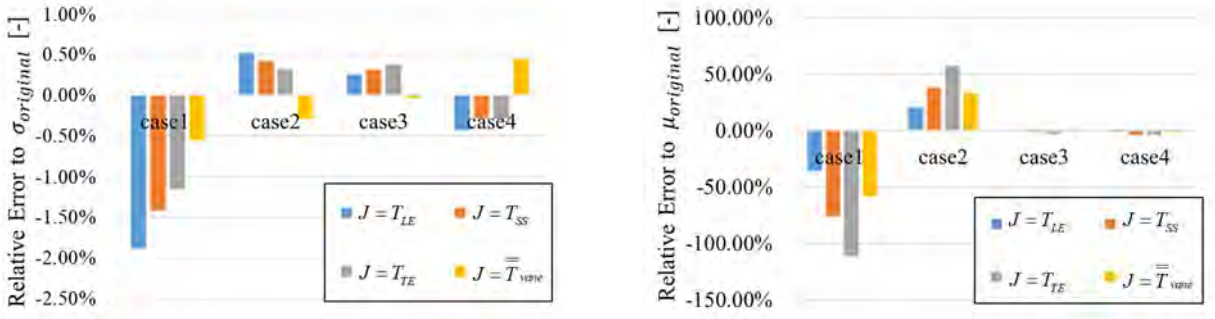


(a) fit coefficients σ in different cases (b) fit coefficients μ in different cases

**Figure 15 Relative error to fit coefficients of original geometry**

Figure 16(a) shows a inlet temperature distributed as a quadratic function as an example and then calculate dJ and the relative error to $dJ_{original}$ as following equations:

$$dT_{BC} = T_{BC} - T_{uniform} = 350 - \frac{1}{2} \times \frac{50}{l/2} y^2 - 300 = 50 - \frac{1}{2} \times \frac{50}{l/2} y^2 \quad (8)$$

$$dJ = \int_{inlet} \frac{\partial J}{\partial T_{BC}} dT_{BC} \quad (9)$$

$$E_{dJ} = \frac{dJ_{case\_i} - dJ_{original}}{dJ_{original}} (i = 1,2,3,4) \quad (10)$$

Figure 16(b) shows: comparing with original geometry, the geometry of case1 increases the heat load under this non-uniform condition although it is more robust to inlet conditions. While case2 decreases the heat load which predicts the thinner suction surface will decrease the temperature under such inlet condition. And there's not much change to the observables in case3 and case4.

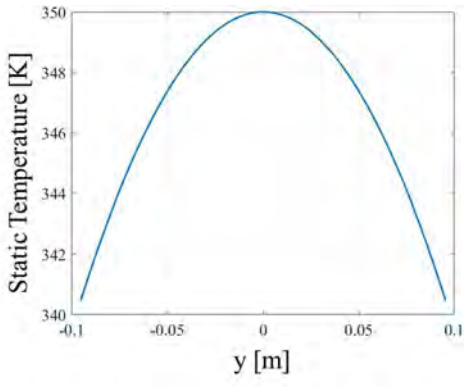


(a) distribution of inlet temperature

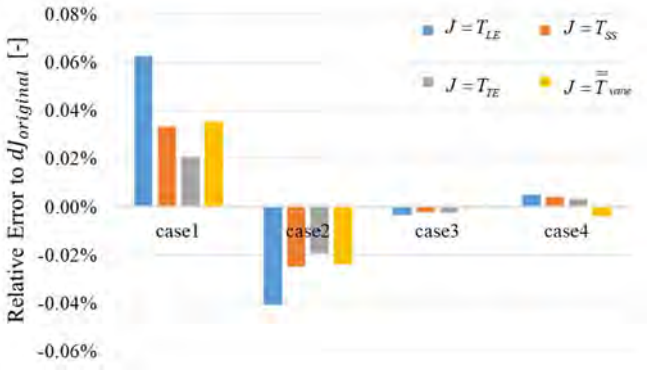


(b) relative error to $dJ_{original}$ in different cases

**Figure 16 Inlet temperature and the prediction results using sensitivity**

Considering the sensitivity to boundary temperature is not enough for vane design, but this study tells us that the sensitivity to boundary temperature can be affected by different vane geometry. If the non-uniform distribution of inlet temperature cannot be changed, a slight adjustment of vane geometry may make the inlet position with high sensitivity avoid the high temperature position, thus decreasing the heat load of the key area of vane.

## CONCLUSION

In this paper, a method is proposed to predict the observed values based on the sensitivity to boundary condition obtained by one adjoint calculation. This method provide a simple way for designing the relative position of non-uniform inlet temperature and vane cascade. The sensitivity information depend on the flow field can advise designer where is more dangerous for the heat load of vane to put a hot streak on the inlet. And the sensitivity can used to compute the value of observable under non-uniform boundary condition, needing only one adjoint calculation instead of many flow calculations. Also the sensitivity information can evaluate the robustness of vane geometry. The accuracy of this method is verified by 2D and 3D cases. The main conclusions are as follows:

1. The sensitivity to boundary temperature as observable $J = \bar{\bar{T}}_{vane}$ does not change with inlet temperature condition. The sensitivity information at uniform inlet can be used to predict J at non-uniform temperature inlet. For a design problem knowing the turbine inlet temperature distribution, the sensitivity information can be used to directly calculate the objective function J, to optimize the matching relationship between inlet conditions and vane passage.

2. There is a corresponding relationship between the shape of sensitivity curve to and inlet flow angle which can be used to obtain the sensitivity curve under different flow angle.

3. In the 3D cases of linear cascade with swirl inlet, the distribution of sensitivity to boundary temperature is significantly different from the uniform inlet condition due to the complexity of the flow fields. But there is still a strong correlation between boundary sensitivity and streamlines. The inlet positions of these particular streamlines (such as the streamlines around vane or composing the vortex) can tell us where are not suitable for placing hot streaks.

4. Sensitivity information can be used to evaluate the robustness to non-uniform inlet temperature of the vane geometry, and give advices for vane designing.

## ACKNOWLEDGEMENT

This work is supported by the National Natural Science Foundation of China [Grant No. 52276031] and National Science and Technology Major Project [J2019-II-0008-0028 ].

## REFERENCES


Simone, Salvadori, Francesco Montomoli, Francesco Martelli, Kam S Chana, Imran Qureshi, and Tom Povey. Analysis on the Effect of a Non-uniform Inlet Profile on Heat Transfer and Fluid Flow in Turbine Stages. Journal of Turbomachinery 134, no. 1 (2012): 11012.

Basol, Altug M, Philipp Jenny, Mohamed Ibrahim, Anestis I Kalfas, and Reza S Abhari. Hot Streak Migration in a Turbine Stage: Integrated Design to Improve Aerothermal Performance. Journal of Engineering for Gas Turbines and Power 133, no. 6 (2011): 61901.

Li, Yifei, Xinrong Su, and Xin Yuan. The Effect of Mismatching between Combustor and HP Vanes on the Aerodynamics and Heat Load in a 1-1/2 Stages Turbine. Aerospace Science and Technology 86 (2019): 78-92.

Feng, Zhenping, Zhaofang Liu, Yan Shi, and Zhiduo Wang. Effects of Hot Streak and Airfoil Clocking on Heat Transfer and Aerodynamic Characteristics in Gas Turbine. Journal of Turbomachinery 138, no. 2 (2016): Journal of Turbomachinery, 2016, Vol.138 (2).

An, Bai-Tao, Jian-Jun Liu, and Hong-De Jiang. Numerical Investigation on Unsteady Effects of Hot Streak on Flow and Heat Transfer in a Turbine Stage. Journal of Turbomachinery 131, no. 3 (2009): 31015-15.

Mansouri, Zakaria, and Richard Jefferson-Loveday. Heat Transfer Characteristics of a High-pressure Turbine under Combined Distorted Hot-streak and Residual Swirl: An Unsteady Computational Study. International Journal of Heat and Mass Transfer 195 (2022): 123143.

Povey, T., Chana, K.S., Jones, T.V. and Hurrion, J., The Effect of Hot-Streaks on HP Vane Surface and Endwall Heat Transfer: An Experimental and Numerical Study.

Jenny, P., C. Lenherr, R. S Abhari, and A. Kalfas. Effect of Hot Streak Migration on Unsteady Blade Row Interaction in an Axial Turbine. Journal of Turbomachinery 134, no. 5 (2012): 51020-9.

Miki, Kenji, Thomas Wey, and Jeffrey Moder. Computational Study on Fully Coupled Combustor–Turbine Interactions. Journal of Propulsion and Power 39, no. 4 (2023): 540-53.

Wang, Tianyi, Yimin Xuan, and Xingsi Han. Investigation on Hybrid Thermal Features of Aero- Engines from Combustor to Turbine. International Journal of Heat and Mass Transfer 200 (2023): 123559.

Peter, Jacques E.V., and Richard P. Dwight. Numerical Sensitivity Analysis for Aerodynamic Optimization: A Survey of Approaches. Computers & Fluids 39, no. 3 (2010): 373-91.

Juan Lu, Chaolei Zhang, Zhenping Feng. Aerodynamic Optimization and Inverse Design of 2D and 3D Turbine Cascades Using the Discrete Adjoint Method. Proc. ASME. GT2013, Volume 6B: Turbomachinery. Paper No: GT2013-95284

Halila, Gustavo L.O., Joaquim R.R.A. Martins, and Krzysztof J. Fidkowski. Adjoint-based Aerodynamic Shape Optimization including Transition to Turbulence Effects. Aerospace Science and Technology 107 (2020): 106243.

Arens, K., P. Rentrop, S.O. Stoll, and U. Wever. An Adjoint Approach to Optimal Design of Turbine Blades. Applied Numerical Mathematics 53, no. 2 (2005): 93-105.

SU, Xinrong, and Xin YUAN. Adjoint Boundary Sensitivity Method to Assess the Effect of Nonuniform Boundary Conditions. Chinese Journal of Aeronautics 35, no. 2 (2022): 12-16.

Zhang, Zhen, Yinbo Mao, Xinrong Su, and Xin Yuan. Adjoint-Based Boundary Condition Sensitivity Analysis. AIAA Journal 60, no. 6 (2022): 3517-527.

Fraser B. Jones, Todd Oliver, and David G. Bogard. Adjoint Optimization of Film Cooling Hole Geometry. Proceedings of ASME Turbo Expo 2021. Virtual, Online. GT2021-59332

Zhang, Yang, Yifei Li, Xiutao Bian, and Xin Yuan. Effects of Inlet Swirl on Pressure Side Film Cooling of Neighboring Vane Surface. Journal of Thermal Science and Engineering Applications 11, no. 6 (2019): Journal of Thermal Science and Engineering Applications, 2019, Vol.11 (6).


.